A Class of Supported Membranes: Formation of Fluid Phospholipid Bilayers on Photonic Band Gap Colloidal Crystals

ARTICLE *in* JOURNAL OF THE AMERICAN CHEMICAL SOCIETY · FEBRUARY 2006

Impact Factor: 12.11 · DOI: 10.1021/ja056701j · Source: PubMed

4 AUTHORS, INCLUDING:

Babak Sanii
The Claremont Colleges
35 PUBLICATIONS **434** CITATIONS

SEE PROFILE

Atul N Parikh
University of California, Davis
175 PUBLICATIONS **6,894** CITATIONS

SEE PROFILE

J|A|C|S
COMMUNICATIONS

Published on Web 12/10/2005

A Class of Supported Membranes: Formation of Fluid Phospholipid Bilayers on Photonic Band Gap Colloidal Crystals

Adrian M. Brozell, Michelle A. Muha, Babak Sanii, and Atul N. Parikh*

Department of Applied Science, University of California, Davis, California 95616

Received October 12, 2005; E-mail: anparikh@ucdavis.edu

Supported membranes,[1] single fluid phospholipid bilayers deposited on solid surfaces, have been of considerable interest as models for biological membranes both for fundamental studies of cell surface mechanisms and for designing biosensors and assays for membrane targets.[2] To this end, many support surfaces now spanning a broad range of oxides (glass, SiO_2, TiO_2, $SrTiO_3$, mica, and oxidized PDMS) and polymeric substrates[3] have proved useful. Although one key application of supported membranes is in designing recognition-specific biomimetic devices, it is notable that examples of supported membranes integrated directly to optical transducers are limited.[4] Here, we report the formation of a new class of supported membranes comprising a fluid phospholipid assembly coupled directly to a broadly tunable colloidal crystal with a well-defined photonic band gap.

Monodisperse colloids (e.g., silica and polystyrene microspheres) spontaneously organize under certain conditions to form 3D face-centered cubic (fcc) lattices on solid substrates.[5] These planar crystals exhibit a periodic spatial variation of refractive index with lattice constants on the order of the wavelength of light, thus exhibiting a well-defined photonic band gap (PBG).[6] The ability to couple membranes with colloidal crystals opens useful optical transduction possibilities for probing membrane-mediated molecular recognition and transport. Furthermore, from the experimental point of view, colloidal crystals offer at least two additional properties of significant interest in fundamental studies of membranes. *First*, the surfaces of colloidal crystals exhibit 2D patterns of curvature in a tunable range (dependent on colloid dimensions), thereby allowing systematic studies of many curvature-dependent properties of lipid membranes.[7] *Second*, the presence of water-filled pores in the interstices between the hydrated colloids provides a much sought-after aqueous transition layer[8] for cushioning the membrane−substrate interface and for functional incorporation of integral membrane proteins.

Recent studies indicate that a favorable interaction between a porous surface and small unilamellar vesicles (SUVs) might exist.[9] These studies show that solid substrates exhibiting nanoscale porosity prompt surface-induced rupture and spreading of vesicles, yielding 2D continuous bilayers spanning the pores. We have produced fluid-supported membranes by rupture and spreading of SUVs onto a variety of colloidal crystals (Figure 1a). Our colloids were organized into a photonic fcc lattice (Figure 1b) by adapting a previously reported physical confinement method.[10] Briefly, a 10−20 μL aliquot of silica colloidal solution near the critical concentration (44−56% v/v) is sandwiched between one hydrophilic and one hydrophobized glass plate and left standing for ∼3 days to allow slow solvent evaporation. Separating the two glass surfaces leaves planar colloidal crystals on the hydrophilic plate. UV/vis spectra (Supporting Information, SI) of the crystals reveal a characteristic dip when in air. When immersed in water, the spectrum shifts by ∼50 nm and narrows as expected,[11] confirming the retention of the band gap. The crystal surfaces were then

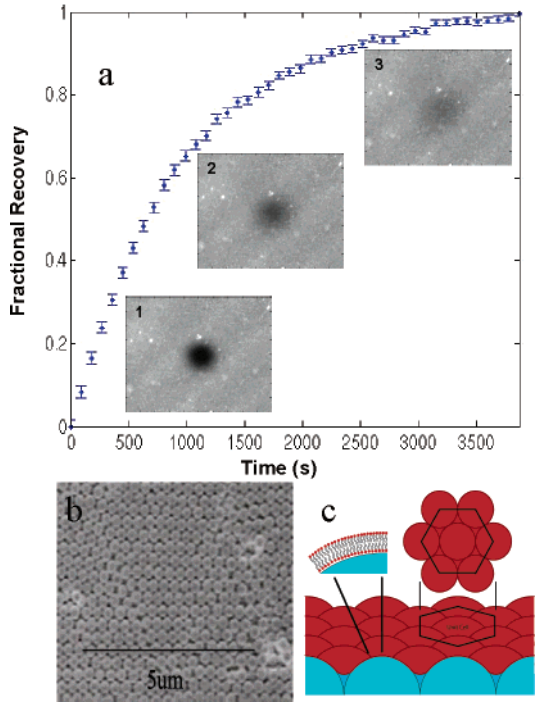

Figure 1. (a) A FRAP fractional recovery plot of a Texas-Red doped POPC bilayer on a 330 nm colloidal crystal. Insets: 200 × 160 μm^2 epifluorescence images of a bleached spot (40 μm diameter) at times, t = 0, 630, and 1530 s. (b) An SEM image of a 330 nm silica colloidal crystal. (c) A cartoon illustrating a bilayer on top of a nanocolloidal crystal.

oxidized using ozone-generating UV radiation (184−257 nm) for ∼30 min. SUVs of ∼110 nm diameter comprising 1-palmitoyl-2-oleoyl-*sn*-glycero-3-phosphocholine (POPC) doped with 1 mol % of fluorescent Texas Red 1,2-dihexadecanoyl-*sn*-glycero-3-phosphoethanolamine triethylammonium salt (TR-DHPE) were fused onto the planar crystals by incubating the substrate with SUV solution for ∼1 h, and excess vesicles were rinsed extensively using deionized water before further characterization (SI).

The bulk of the characterization discussed below has focused on two classes of colloidal crystals: fcc lattices of nanoscale (330 nm) and microscale (5.66 μm) silica microspheres. The observed bright and homogeneous fluorescence signal (Figure 1d insets and SI) indicates the formation of a laterally uniform POPC bilayer on a 330 nm colloidal crystal. Despite the presence of interparticle interstices, trapping of unfused vesicles is not observed. The long-range fluidity of these bilayers is established using fluorescence recovery after photobleaching (FRAP) measurements[12] (Figure 1d), which indicate 2D continuous bilayer spanning multiple beads. In contrast, when larger (5.66 μm) beads are used, neither the long-range fluidity nor the homogeneous deposition occurs. Instead, a fluorescence pattern revealing the crystal lattice is seen, which does not display long-range lateral fluidity in FRAP studies (SI). This

10.1021/ja056701j CCC: $33.50

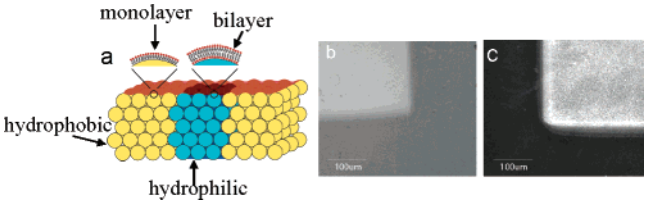

Figure 2. (a) A cartoon illustrating spatially patterned columns of hydrated, hydrophilic colloids (blue) in hydrophobic surroundings (yellow) of a colloidal crystal. (b) A 10X bright-field image of UV-patterned OTS-coated 330 nm silica crystal in water. The darker region corresponds to an unhydrated, OTS-coated region (band gap ~ 605 nm), and the brighter region is the hydrated region (band gap ~ 658 nm). (c) A 10X fluorescence image of a TR-DHPE doped POPC bilayer on a patterned colloidal crystal.

apparent discrepancy in the vesicle spreading behavior appears to be related to the relative sizes of the SUVs and that of the interstices between the colloids: 100 nm SUVs cannot permeate through the interstitial space (estimated to be ≤49.5 nm) between 330 nm beads and thus rupture across multiple beads. However, with 5.6 μm beads, the same SUV could pass through the interstitial space and "wet" the crystal interior. This steric argument suggests the existence of a relationship between colloidal and vesicles diameters, which determines the vesicle spreading behavior. We note that the bilayer deposition does not change the band gap characteristics of the colloidal crystal.

Adapting a rigorous data analysis protocol first developed by Axelrod et al.[12] (SI), we estimate a 2D projected probe diffusion coefficient of 2.1(±0.4) × 10^{-9} cm^2/s with a fractional mobility of 74.3(±0.3)% for POPC bilayers (doped with TR-DHPE) spread over 330 nm colloidal crystals. By comparison, a bilayer on clean coverglass yields higher values of 8−12 × 10^{-9} cm^2/s by our method of analysis. To better understand the observed quantitative disparity in probe diffusion characteristics, we consider two factors. *First*, the membrane can be expected to roughly follow the colloidal topology due to a strong adhesion between membrane and glass. Effective surface area due to spherical caps is ~91% larger than the corresponding flat topography,[13] possibly partially accounting for the lower FRAP recovery rates. *Second*, for the nanoscale colloids, the high bending penalty competes with the glass−membrane adhesion energy,[14] presumably resulting in an optimal bilayer folding pattern. This imposition of periodic arrays of curvatures on the bilayer may result in spatially varying lipid packing densities, thus impacting bilayer diffusional properties on the colloidal crystals.

Next, we show that a spatial control of crystal wettability allows the creation of binary patterns of band gaps and corresponding patterns of lipid morphologies (Figure 2). We used *n*-octadecyltrichlorosilane (OTS) self-assembly to render the crystal water-repellent. When submerged in water, the PBG does not shift or narrow as it does for hydrophilic crystals (SI). These hydrophobic colloidal crystals can then be spatially patterned using a simple UV/ozone treatment in conjunction with a physical mask to produce corresponding binary patterns of wettability. When vesicles are *incubated with* these patterned surfaces, single homogeneous bilayers and monolayers form on hydrophilic and hydrophobic regions, respectively,[15] "epitaxially" reflecting the underlying pattern of band gaps and substrate wettabilities.[15] We expect that such constructs juxtaposing alternating monolayers and bilayers on PBG patterns will be useful for parallel assays of membrane functions that require both leaflets (e.g., ion-channel-induced transport).

In summary, a fluid lipid bilayer can be supported by a colloidal crystal with a well-defined photonic band gap. An interplay between vesicle sizes and the interstices between the colloidal particles determines the spreading behavior. For nanoscale beads, the bilayer spreads as a two-dimensionally contiguous sheet covering the crystal surface. This configuration should enable future studies of membrane transport, such as by ion channels, by monitoring shifts in band gaps of nanoscale crystals. For the microscale colloidal crystals, where each colloid is individually wrapped by a bilayer, accessible membrane per unit projected area is significantly enhanced. We envisage optical assays of recognition properties of membranes utilizing this construct.

Acknowledgment. We gratefully acknowledge Drs. A. Sapuri-Butti and S. Dixit for discussions. We thank the Office of Science, Department of Energy (DE-FG02-04ER46173), NSF Center for Biophotonics Science and Technology (PHY 0120999), and Graduate Summer Fellowship (B.S.) for funding.

Supporting Information Available: Details of FRAP data analysis method, data supporting the absence of long-range lateral mobility in membranes supported on microscale beads, and UV−visible spectra confirming band gap properties of colloidal crystals. This material is available free of charge via the Internet at http://pubs.acs.org.

References

(1) (a) Tamm, L. K.; McConnell, H. M. *Biophys. J.* **1985**, *47*, 105−113. (b) Sackmann, E. *Science* **1996**, *271*, 43−48.

(2) (a) Groves, J. T. *Curr. Opin. Drug Discovery Dev.* **2002**, *5*, 606−612. (b) Cornell, B. A.; Braach-Maksvytis, V. L. B.; King, L. G.; Osman, P. D. J.; Raguse, B.; Wieczorek, L.; Pace, R. J. *Nature* **1997**, *387*, 580−583. (c) Schuster, B.; Gufler, P. C.; Pum, D.; Sleytr, U. B. *IEEE Trans. Nanobiosci.* **2004**, *3*, 16−21.

(3) See, for example: (a) Munro, J. C.; Frank, C. W. *Langmuir* **2004**, *20*, 10567−10575. (b) Rossetti, F. F.; Bally, M.; Michel, R.; Textor, M.; Reviakine, I. *Langmuir* **2005**, *21*, 6443−6450. (c) Starr, T. E.; Thompson, N. L. *Langmuir* **2000**, *16*, 10301−10308.

(4) Brake, J. M.; Daschner, M. K.; Luk, Y. Y.; Abbott, N. L. *Science* **2003**, *302*, 2094−2097.

(5) (a) Xia, Y. N.; Gates, B.; Yin, Y. D.; Lu, Y. *Adv. Mater.* **2000**, *12*, 693−713. (b) Fudouzi, H.; Lu, Y.; Xia, Y. N. In *Chromogenic Phenomena in Polymers*; Jenekhe, S. A., Kiserow, D. J., Eds.; ACS Symposium Series 888; American Chemical Society: Washington, DC, 2005. (c) Ozin, G. A.; Yang, S. M. *Adv. Funct. Mater.* **2001**, *11*, 95−104.

(6) (a) Yablonovitch, E. *Phys. Rev. Lett.* **1987**, *58*, 2059−2062. (b) Joannopoulos, J. D.; Villeneuve, P. R.; Fan, S. H. *Nature* **1997**, *386*, 143−149.

(7) See, for example: (a) Huttner, W. B.; Zimmerberg, J. *Curr. Opin. Cell Biol.* **2001**, *13*, 478−484. (b) Julicher, F.; Lipowsky, R. *Phys. Rev. Lett.* **1993**, *70*, 2964−2967.

(8) (a) Wagner, M. L.; Tamm, L. K. *Biophys. J.* **2000**, *79*, 1400−1414. (b) Sackmann, E.; Tanaka, M. *Trends Biotechnol.* **2000**, *18*, 58−64.

(9) (a) Weng, K. C.; Stalgren, J. J. R.; Duval, D. J.; Risbud, S. H.; Frank, C. W. *Langmuir* **2004**, *20*, 7232−7239. (b) Gufler, P. C.; Pum, D.; Sleytr, U. B.; Schuster, B. *Biochim. Biophys. Acta* **2004**, *1661*, 154−165. (c) Ogier, S. D.; Bushby, R. J.; Cheng, Y. L.; Evans, S. D.; Evans, S. W.; Jenkins, A. T. A.; Knowles, P. F.; Miles, R. E. *Langmuir* **2000**, *16*, 5696−5701. (d) Hennesthal, C.; Steinem, C. *J. Am. Chem. Soc.* **2000**, *122*, 8085−8086.

(10) Park, S. H.; Qin, D.; Xia, Y. *Adv. Mater.* **1998**, *10*, 1028−1031.

(11) Tarhan, I. I.; Watson, G. H. *Phys. Rev. B* **1996**, *54*, 7593−7597.

(12) Axelrod, D.; Koppel, D. E.; Schlessinger, J.; Elson, E.; Webb, W. W. *Biophys. J.* **1976**, *16*, 1055−1069.

(13) This calculation assumes strict adhesion between the membrane and the spherical caps, separating only at the equator. It also assumes that the spheres are touching.

(14) (a) Swain, P. S.; Andelman, D. *Phys. Rev. E* **2001**, 6305. (b) Swain, P. S.; Andelman, D. *Langmuir* **1999**, *15*, 8902−8914.

(15) Howland, M. C.; Sapuri-Butti, A. R.; Dixit, S. S.; Dattelbaum, A. M.; Shreve, A. P.; Parikh, A. N. *J. Am. Chem. Soc.* **2005**, *127*, 6752−6765.

JA056701J